The final publication is available at

https://doi.org/10.1016/j.cmpb.2022.106934

Additional Information

Considering Population Variability of Electrophysiological Models Improves the *In Silico* Assessment of Drug-Induced Torsadogenic Risk

1   Jordi Llopis-Lorente, Beatriz Trenor[†] and Javier Saiz[†*]

2   *Centro de Investigación e Innovación en Bioingeniería (Ci²B), Universitat Politècnica de*

3   *València, camino de Vera, s/n , 46022, Valencia, Spain.*

4   [†] These authors contributed equally to this work

5   *** Corresponding author:**

6   Javier Saiz

7   email: jsaiz@ci2b.upv.es

8   Phone: +34 96 3877 00 (extension 76025)

11 **Abstract**

12 *Background and Objective: In silico* tools are known to aid in drug cardiotoxicity

13 assessment. However, computational models do not usually consider electrophysiological

14 variability, which may be crucial when predicting rare adverse events such as drug-

15 induced Torsade de Pointes (TdP). In addition, classification tools are usually binary and

16 are not validated using an external data set. Here we analyze the role of incorporating

17 electrophysiological variability in the prediction of drug-induced arrhythmogenic-risk,

18 using a ternary classification and two external validation datasets.

19 *Methods:* The effects of the 12 training CiPA drugs were simulated at three different

20 concentrations using a single baseline model and an electrophysiologically calibrated

population of models. 9 biomarkers related with action potential (AP), calcium dynamics

and net charge were measured for each simulated concentration. These biomarkers were

used to build ternary classifiers based on Support Vector Machines (SVM) methodology.

Classifiers were validated using two external drug sets: the 16 validation CiPA drugs and

81 drugs from CredibleMeds database.

Results: Population of models allowed to obtain different AP responses under the same

pharmacological intervention and improve the prediction of drug-induced TdP with

respect to the baseline model. The classification tools based on population of models

achieve an accuracy higher than 0.8 and a mean classification error (MCE) lower than 0.3

for both validation drug sets and for the two electrophysiological action potential models

studied (Tomek et al. 2020 and a modified version of O'Hara et al. 2011). In addition,

simulations with population of models allowed the identification of individuals with

lower conductances of I_{Kr}, I_{Ks}, and I_{NaK} and higher conductances of I_{CaL}, I_{NaL}, and I_{NCX},

which are more prone to develop TdP.

Conclusions: The methodology presented here provides new opportunities to assess drug-

induced TdP-risk, taking into account electrophysiological variability and may be helpful

to improve current cardiac safety screening methods.

1   Introduction

Drug-induced Torsade de Pointes (TdP) is a special form of polymorphic ventricular

tachycardia. It is one of the most frightening adverse drug reactions because it can

precipitate ventricular fibrillation and cause sudden death. Although it is a rare adverse

event, accounting for less than one case out of 100,000 exposures, several compounds,

including antidepressants, pain medications, antihistamines, etc., have been withdrawn

from the market because of their risk of inducing TdP [1,2]. Over the last years, new

45   strategies for the assessment of drug induced TdP-risk have been proposed with the aim

46   of complementing and improving current regulatory guidelines [3]. One remarkable

47   example is the Comprehensive In Vitro Proarrhythmia Assay (CiPA) initiative, which

48   considers that *in silico* simulations of proarrhythmic effects for different compounds are

49   essential to improve arrhythmogenicity prediction.

50   Most of the mathematical and biophysical cardiac models used in *in silico* studies

51   typically represent the average behavior of a group of cells characterized experimentally.

52   Therefore, these models do not take into account electrophysiological variability [4].

53   However, it is well-known that identical pharmacological interventions produce different

54   responses between individuals. When taking a certain drug, most of the individuals may

55   not suffer any side effects while some of them may undergo TdP. For this reason,

56   accounting for electrophysiological variability may help better estimate drug-induced

57   proarrhythmicity. A useful strategy to account for variability in *in silico* models are

58   population of models [5,6]. Briefly, to build a population of models, a certain number of

59   model parameters are randomly varied, generally the conductance of different ion

60   channels, thus creating a variety of cellular behaviors.

61   Other limitations of some *in silico* classifications tools that have been published are

62   that: i) they are usually based on two-class categorization systems (TdP+ and TdP-), and

63   ii) they use cross-validation methods (e.g., leave-one-out-cross-validation), in which the

64   data used to train the model are also used to validate the model. The White Paper

65   published by Li and colleagues [7] recommends the use of a three-class system (high-

66   risk, intermediate-risk, and low-risk), which represents a compromise between

67   quantitative and qualitative risk assessment. First non-binary *in silico* drug induced TdP-

68   risk classifier was published by Mirams and colleagues[8] in 2011, but since then few

69   non-binary pro-arrhythmic classifiers have been proposed. Furthermore, the White Paper

also stresses that a validation of the tool with a "hidden" test data set, i.e. data not used during the training phase, provides higher confidence on the performance of the tool. To the best of our knowledge, there are only two studies that follow these two principles published to date: a publication by Li and co-workers [9], which uses the "torsade metric score" to classify 16 drugs according to their TdP-risk; and a work by Yoo and collaborators [10], which proposes an artificial neural network using nine features related with charge, action potential, and calcium transient morphology.

The aim of this study is to analyze the role of incorporating electrophysiological variability in the prediction of drug-induced arrhythmogenic-risk. Specifically, the effects of the 12 training CiPA drugs are simulated on a single baseline model and on an electrophysiologically calibrated population of models. Ternary classifiers are built using biomarkers extracted from the simulations of these 12 drugs and are validated with the result from the simulations of 2 drugs datasets: one containing the 16 validation CiPA drugs and the other containing 81 drugs from CredibleMeds. In addition, to evaluate the influence of the action potential model, the same strategy was performed using two different action potential models.

2   Materials and Methods

2.1   *In Silico* population of models

The electrophysiological characteristics of human ventricular cells were simulated taking as reference two of the latest human endocardial ventricular action potential (AP) models: the model published by Tomek and colleagues [11] (TorORd) with the dynamic intracellular chloride and a modified version of the widely used AP model developed by O'Hara's group [12] (ORdmD). The modifications applied to the O'Hara et al. model are described in a previous study [13]. In short, model modifications include the modulation of six channel conductances (I_{Kr} multiplied by a factor of 1.119, I_{Ks} by 1.648, I_{K1} by 1.414,

95   I_{CaL} by 1.018, I_{NaL} by 2.274, and I_{Na} by 0.4) and a reformulation of the activation and

96   inactivation gates of I_{Na}. These modifications were designed to better reproduce

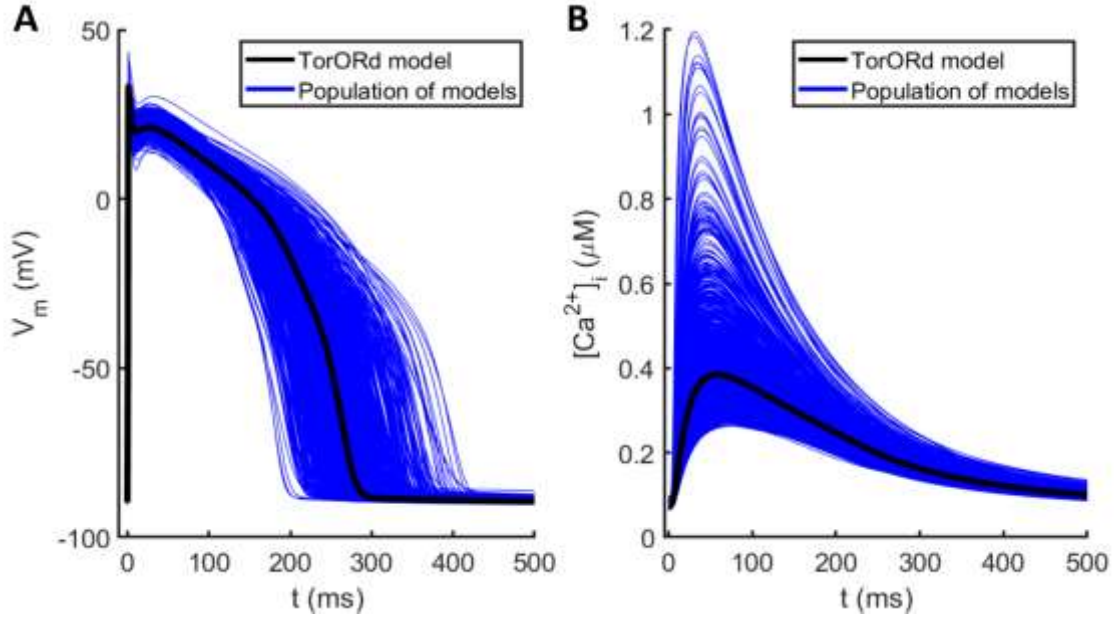97   experimental data on drug effects.

98   To account for electrophysiological variability, two populations of models were built

99   using the aforementioned models as a template. The methodology for constructing the

100 population was the same for both models. First, an initial population of 1,000 models was

101 generated. These models were obtained by randomly and simultaneously modifying the

102 conductances of the ionic currents of the AP model (15 parameters in the case of ORdmD

103 and 17 in the case of TorORd). These scale factors modifying the channel conductances

104 were randomly sampled from a normal distribution with mean 1 and standard deviation

105 0.2, thus assuring that the majority of the population (>99%) was in a range between

106 ±60% with respect to the baseline model. To model non-diseased healthy

107 cardiomyocytes, the results of previous modelling studies [14,15] suggest that a variation

108 bigger than ±50% in conductance values (from the value of the parameter in the baseline

109 model) would allow substantial variability.

110   After running the simulations using the initial populations in control conditions, a

111 calibration was performed. Models with electrophysiological biomarkers not fulfilling the

112 calibration requirements were discarded. Plausible electrophysiological properties were

113 defined according to acceptable ranges, found in the literature, for 15 characteristics

114 related to AP duration, amplitude of membrane potential, and calcium dynamics

115 [6,12,16–20]. Limits of acceptance for the 15 electrophysiological properties considered

116 are shown in **Table 1**. Simulations were run at 37ºC and at the following extracellular

117 concentrations: $[Na^+]$=140 nM, $[Ca^{2+}]$=1.8 nM and $[K^+]$=5.4 nM in order to replicate the

118 experimental conditions of the in vitro experiments.

119 **Table 1.** Action Potential and Ca^{2+}-related biomarkers ranges used to calibrate the control
120 population of human ventricular AP *in silico* models.

Biomarker	Min Value	Max Value
APD40 (ms) [6]	85	320
APD50 (ms) [6]	110	350
APD90 (ms) [6]	180	440
Tri 90-40 (ms) [6,12]	50	150
dV/dt (mV/ms) [12]	150	1000
Vpeak (mV) [6,12]	10	55
RMP (mV) [6,12]	-95	-80
CTD50 (ms) [20]	120	420
CTD90 (ms) [20]	220	785
Ca^{2+} syst (µM) [17]	0.262	2.23
Ca^{2+} diast (µM) [17]	--	0.40
Na^+ (mM) [19]	--	39.27
ΔAPD90 (%) under 90% I_{Ks} [12]	-54.4	62
ΔAPD90 (%) under 70% I_{Kr} [18]	32.25	91.94
ΔAPD90 (%) under 50% I_{K1} [16]	-5.26	14.86

121   After calibration, 810 models of the TorORd-based population and 860 models of the

122 ORdmD-based population presented a plausible electrophysiological behavior according

123 to experimental data. AP and calcium transient traces of the TorORd-based population

124 are shown in **Figure 2**. As shown in the Figure the population of models presents

125 electrophysiological variability. For example, the APD_{90} of the baseline model yields

126 272.25 ms, and the population of models presents APD_{90}s varying between 185.78 and

127 406.3 ms. This electrophysiological variability can also be observed in calcium dynamics,

128 where systolic $[Ca^{2+}]$ varies between 0.263 µM and 1.195 µM. The ORdmD population

129 is shown in the **Supplementary Material, Figure S1**. Distributions of the biomarkers

130 used for calibration across each population of models (TorORd and ORdmD) are

131 represented in **Figure S2 and S3**.

132
133 **Figure 1.** Action potentials (A) and calcium transient (B) traces of the calibrated
134 population (810 models). Solid black lines represent TorORd baseline model.

135 **2.2   Drug Data Set and Drug Effect Simulation**

136   Drug effects on the AP were simulated via the simple pore block model. Thus, the block

137 produced on each current was simulated by scaling the channel's maximal conductance

138 (g_i). This scaling factor was calculated using the standard Hill equation (eq. 1):

$$g_{i,drug} = g_i \left[1 + \left(\frac{D}{IC_{50,i}} \right)^h \right]^{-1} \tag{1}$$

139   where $g_{i,drug}$ is the maximal conductance of channel i in the presence of the drug, D

140 is the drug concentration, $IC_{50,i}$ is the half-maximal response dose for that drug and

141 current through channel i and h is the Hill coefficient, which indicates the number of

142 molecules of drug that are assumed to be sufficient to block one ion channel.

143   In this work we considered drug effects on the seven ionic currents selected by the Ion

144 Channel Working Group of the CiPA initiative [21]. These currents play the most

145 important role in the generation of the AP and cardiac arrhythmias (I_{Na}, I_{NaL}, I_{Kr}, I_{to}, I_{CaL},

146 I_{K1}, and I_{Ks}).

7

147   Here, we study and assess the proarrhythmic-risk of the 28 CiPA drugs [21] and an

148   extra set of 81 drugs. The IC_{50} values, Hill coefficients (h) and human effective free

149   therapeutic plasma concentrations (EFTPC) for each drug were obtained following the

150   methodology described in previous studies [13,22]. In summary, for each value data were

151   collected from public databases and from the scientific literature and the median value

152   (i.e., the center of the distribution of all published data) was selected. Therefore, previous

153   drug datasets [13,22] were reviewed and updated with recently published data. The

154   EFTPC, IC_{50}, and Hill coefficient values for the 109 drugs are listed in the

155   **Supplementary Material**, **Table S1**.

156   Each drug was simulated at three different concentrations: at the EFTPC, at 5 times

157   EFTPC, and at 10 times EFTPC. All simulations were carried out with a basic cycle length

158   (BCL) of 1000 ms and a stimulus of 1.5-fold the diastolic threshold amplitude and a

159   duration of 0.5 ms. The measurements of the biomarkers were done after 500 beats

160   starting from control -no drug- initial values. Differences between biomarkers measured

161   on two consecutives beats at this point was less than 0.5%. At each concentration, 9

162   biomarkers related to TdP-induction risk were measured: action potential duration at 90%

163   repolarization (APD90), triangulation 90-30, triangulation 90-50, net charge throughout

164   the AP (qNet) [23], systolic and diastolic intracellular calcium concentration, calcium

165   transient duration at 90% and 50% repolarization (CTD90 and CTD50), and the

166   electromechanical window (EMw), defined as CTD90-APD90 [24].

167   A repolarization abnormality was defined as either: i) an Early After Depolarization

168   (EADs), i.e. any event with a positive voltage gradient (dV/dt > 0 mV/ms) after 100 ms

169   from the beginning of the AP; ii) a repolarization failure, i.e. the membrane voltage at the

170   end of the beat being higher than resting membrane voltage (Vm > -40 mV); or iii) any

171   event with a positive calcium transient gradient (dCa2+/dt > 0 nM/ms) after 300 ms from

172   the beginning of the AP.

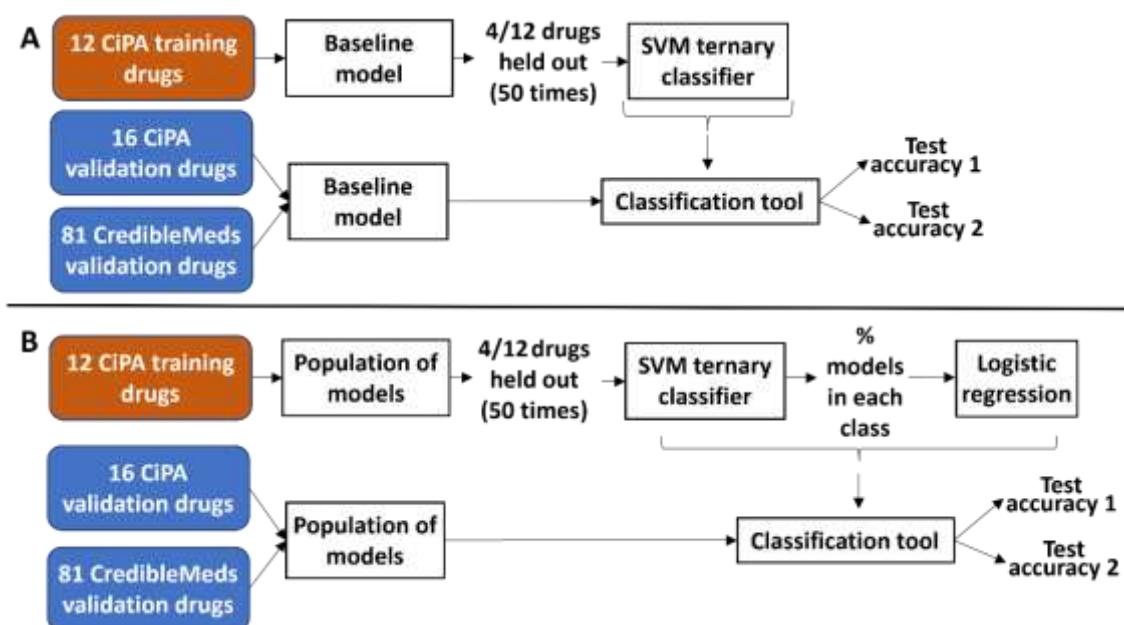173   **2.3   Drug-Induced TdP-Risk Assessment**

174   For the assessment of drug-induced TdP-risk we followed the same methodology for

175   both AP models (ORdmD and TorORd). First, the 12 training CiPA drugs were simulated

176   at three different concentrations using both: the baseline model and the population of

177   models. As mentioned before, at each concentration, 9 biomarkers were measured,

178   therefore the drug effect was characterized by 27 parameters in each model. In the case

179   that a repolarization abnormality occurred during the last 3 beats, none of the biomarkers

180   was measured and it was considered that the drug, for that specific model, poses high risk

181   of inducing TdP.

182   Using these 27 biomarkers as input, two ternary classifiers (high-risk, intermediate-

183   risk, and low-risk) were built: one for the baseline model and the other one for the

184   population of models. In both cases, a ternary Support Vector Machines (SVM) model

185   with a 1/3 hold out cross-validation was trained. For the training phase only the

186   simulations of the 12 training CiPA drugs were used. For the SVM hyperparameters

187   optimization, leave-p-out cross-validation (being p equal to a third of all the training

188   simulations) was performed with 50 bootstrap repetitions, i.e., the training phase was

189   repeated 50 times to avoid the influence of data partitioning. For the training of the

190   classifier using the population of models, the cross-validation was applied using all the

191   drugs on all models of the population (i.e. the number of training points was: 8 drugs*

192   number of models of the population).

193   In the case of the population of models, for each drug, the percentage of models or

194   individuals that are classified as high, as intermediate, or as low-risk was calculated. Next,

195 to determine the risk category of the drug, two logistic regression (one for high-vs.-no

196 high-risk prediction and other for low-vs.-no low-risk prediction) was applied on these

197 percentages. This way, the classification tool built using the population of models yields

198 the TdP-risk category of the drug, associated with the percentage of models in each

199 category.

200 **Figure 2** shows a schematic representation of the overall method for constructing the

201 baseline model-based classifier (**Figure 2A**) and the population of models-based

202 classifier (**Figure 2B**)

203
204 **Figure 2.** Schematic representation of the overall method to build the classifiers. (A)
205 Baseline model-based classifier: the 12 CiPA training drug effects were simulated in the
206 baseline model, then a SVM with 4 drugs held out was trained. (B) Population of models-
207 based classifier: the 12 CiPA training drug effects were simulated in the population of
208 models and a SVM with 4 drugs held out was trained. The percentage of that are classified
209 as high, as intermediate, or as low-risk was used as input of a logistic regression model
210 to determine the overall risk category of the drug. Both classification tools were tested
211 with two external datasets.

212 The TdP-risk classifiers were built and evaluated using the Statistics and Machine

213 Learning Toolbox from MATLAB, version R2021b. The SVM kernels and

214 hyperparameters were tuned using the Bayesian Optimization algorithm. We tested three
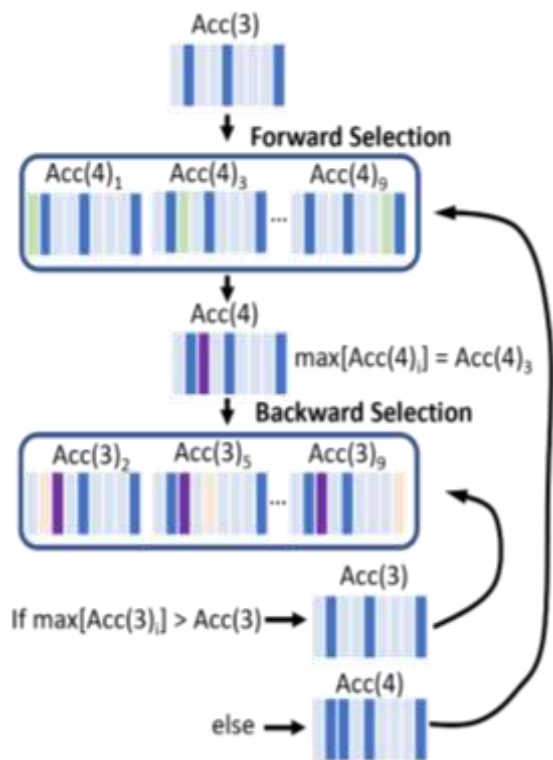
215   kernel functions: Gaussian, linear and polynomial. The margin C was selected from the

216   range $[10^{-4}, 10^4]$. For the Gaussian kernel, the gamma parameter tested ranged from $[10^{-4},$

217    $10^4]$. The polynomial order evaluated ranged from $[2, 5]$. The final SVM configuration

218   for the different classifiers presented in this work are reported in **Table S4**.

219   For visual interpretation of the classification results in the population, we defined a

220   TdP-score. The TdP-score was calculated as the value of the high-vs.-no high-risk

221   regression model minus the value of the low-vs.-no low-risk regression model. This score

222   was normalized between 1 and -1. Thus, TdP-score ranges from 1 when all models are

223   predicted as high-risk or -1 when all models are predicted as low-risk.

224   Once the classifiers were built, both classifiers were tested using two different external

225   datasets: 1) the 16 validation CiPA drugs; 2) 81 drugs whose torasodgenic-risk was taken

226   from CredibleMeds [25]. CredibleMeds defines 4 TdP-risk categories, so in this work,

227   for the evaluation of the ternary classifiers, we considered: class 1 ("known risk of TdP")

228   as high-risk; class 2 ("possible risk of TdP") and class 3 ("conditional risk of TdP") as

229   intermediate-risk; and class 4 ("no known risk of TdP") as low-risk.

230   Finally, a feature selection algorithm was applied to reduce the number of needed

231   biomarkers. Specifically, a sequential forward floating search (SFFS) algorithm [26] was

232   used to identify the best subset of features differentiating the three TdP-risk categories. A

233   feature was considered as a certain biomarker, for example APD90, at the three different

234   concentrations. Therefore, the total number of biomarkers on which the SFFS algorithm

235   was applied was 9. In brief, starting from an empty set of features, the feature X_i that

236   maximizes the accuracy of the classifier when combined with the features Y_k that have

237   been previously selected, is added. After this forward step, SFFS performs backward

238 steps, removing features, provided that the objective function increases. A schematic

239 representation of the algorithm is shown in **Figure 3**.

240
241 **Figure 3.** Schematic representation of the SFFS algorithm, based on Corino et al. [27].
242 Each group of 9 bars represents the whole set of features, being a bar a feature. Each dark
243 blue bar represents a chosen feature. Here, as an example, the algorithm starts with three
244 features already selected that yield an accuracy Acc(3). Then, in the Forward Selection
245 block a new feature is added (colored in green) and the corresponding accuracy measured
246 ($Acc(4)_i$). Not yet selected features are colored in light blue. The feature leading to the
247 maximum accuracy is added to the selected set of features (purple bar). Following is the
248 Backward Selection block, where each of the already selected features (except the last
249 added) is removed (beige bar) from the set of selected features and the corresponding
250 accuracy is computed ($Acc(3)_i$). It the maximum accuracy $Acc(3)_i$ is bigger than the first
251 Acc(3), then the feature is removed from the set of selected features. In case a feature is
252 removed, Black Selection block is repeated, otherwise the next step is Forward Selection.

253   Population of models parameter sets, the ORdmD CellML file and MALTAB code used

254 in this work are available at: https://riunet.upv.es/handle/10251/182593

255 **3   Results**

256 **3.1 Variability in drug response**

257   The population of models produces electrophysiological variability when simulating

258 drug effects. As shown in **Figure 4**, the same pharmacological intervention, in this case

259   10 times EFTPC of vandetanib (high TdP-risk drug), droperidol (intermediate TdP-risk

260   drug) or metoprolol (low TdP-risk drug), have very different effects throughout the

261   population of TorORd models. For example, in the case of vandetanib there are some

262   models, such as models number 32, 199, and 293, that prolong APD less than 40% with

263   respect to control conditions, while others prolong it more than 130% or even develop

264   repolarization abnormalities. These differences cannot be captured with the baseline
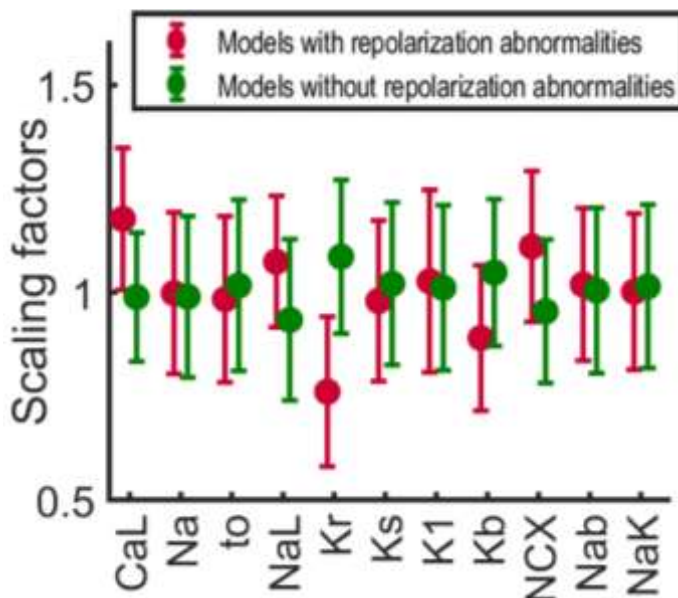
265   model.

266
267 **Figure 4.** Action potential traces of the calibrated population of models under vandetanib
268 effect, a high TdP-risk drug (red lines), under droperidol effect, an intermediate TdP-risk
269 drug (yellow lines) and metoprolol. Baseline model results for each drug are plotted in
270 black lines. The drug concentration is 10 times EFTPC.

271   Repolarization abnormalities observed across the simulations included early

272   afterdepolarizations and repolarization failure. No depolarization failure nor delay

273   afterdepolarizations were detected. Abnormalities in Ca^{2+} transient which did not affect

274   the action potential were not observed either.

275   The analysis of the population subgroups highlighted the ionic properties of those

276   models more prone to develop repolarization abnormalities under the effects of different

277   drugs. The most susceptible TorORd models presented significantly lower conductances

278   of I_{Kr}, and I_{Kb}, and higher conductances of I_{CaL}, I_{NaL} and I_{NCX}. **Figure 5** shows the mean

279   scaling factor values of the different ionic conductances for the TorORd-models

280   developing repolarization abnormalities and the TorORd-models without repolarization

281   abnormalities. This information could be useful to further investigate and establish

282   clusters of patients in which the dose of proarrhythmogenic drugs should be avoided or

283   reduced. For example, patients with cardiovascular pathologies, such as heart failure,

284   hypertrophic cardiomyopathy or ischemic cardiopathy, undergo a ionic remodeling

285   process in which conductances of I_{Kr} and I_{NaK} decrease and conductances of I_{CaL} and I_{NCX}

286   increase [20,28,29], thus increasing their risk of suffering a drug-induced TdP. These

287   patients require special attention in cardiac safety studies and high TdP-risk drugs should

288   be administered with caution.

289

290 **Figure 5.** Mean scaling factor values of the different ionic conductances for the TorORd-
291 models developing repolarization abnormalities (in red) and the TorORd-models without
292 repolarization abnormalities (in green).

293   ORdmD-based simulations produced similar results. Individuals with greater

294   probability of developing repolarization abnormalities also showed higher conductance

295   values of I_{CaL}, I_{NaL}, and I_{NCX}, and lower I_{Kr}. ORdmD-subpopulation did not show

296   significant differences in terms of I_{Kb}. This may be explained because I_{Kb} conductance is

297   more than 6 times higher in TorORd model, so its contribution to the AP is higher. On

14

298   the other hand, ORdmD-subpopulations show lower conductances of I_{Ks} and I_{NaK}. Mean

299   scaling factor values of the different ionic conductances for the ORdmD models

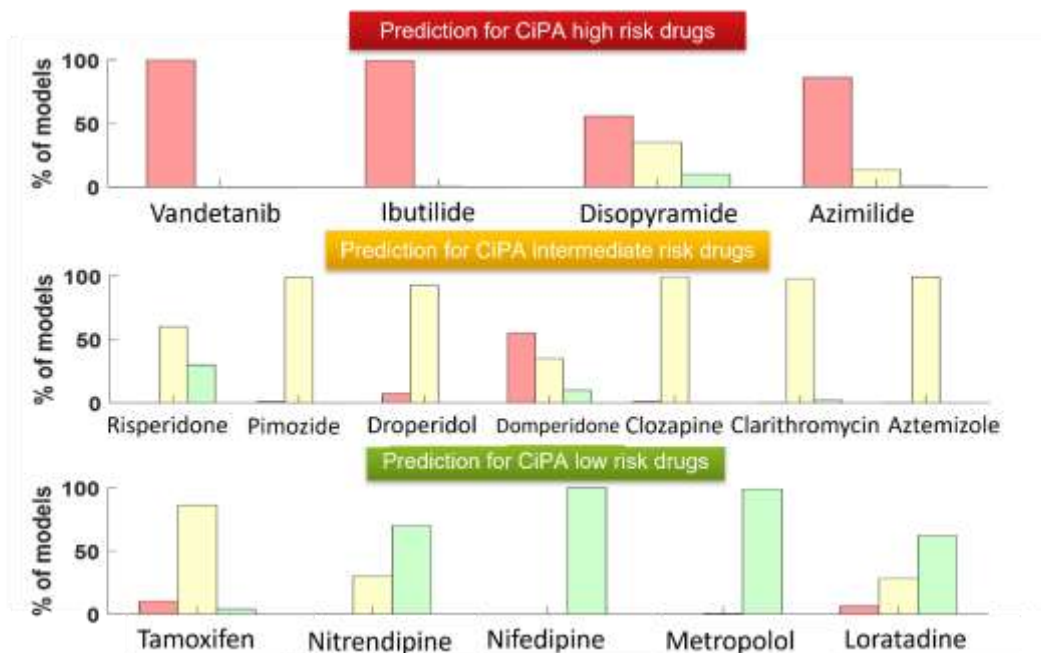300   depending on the presence of repolarization abnormalities are shown in **Figure S4**.

301   **3.2   TdP-risk classifiers**

302   Next, the simulations of the 12 training CiPA drugs were used to train two TdP-risk

303   classifiers: one using the baseline model and the other classifier using the population of

304   models to account for electrophysiological variability. Then, the classification tool was

305   tested using two different external data sets: the 16 validation CiPA drugs and 81

306   CredibleMeds drugs.

307   Here we present the result of the simulations based on TorORd model, since it yields

308   slightly superior results than ORdmD. For the results of the simulations based on the

309   ORdmD model see the **Supplemental Materials** (**Tables S2** and **S3**, **Figures S5 and**

310   **S6**). Note, that the same methodology was followed for both AP models simulations

311   (TorORd and ORdmD).

312   **Figure 6** shows, for the 16 validation CiPA drugs, the percentage of models of the

313   TorORd population that the SVM classifies in each of the three TdP-risk categories. It

314   can be observed, that for some drugs as disopyramide, tamoxifen, or loratadine, the

315   different individuals of the population are assigned to the three TdP-risk categories. This

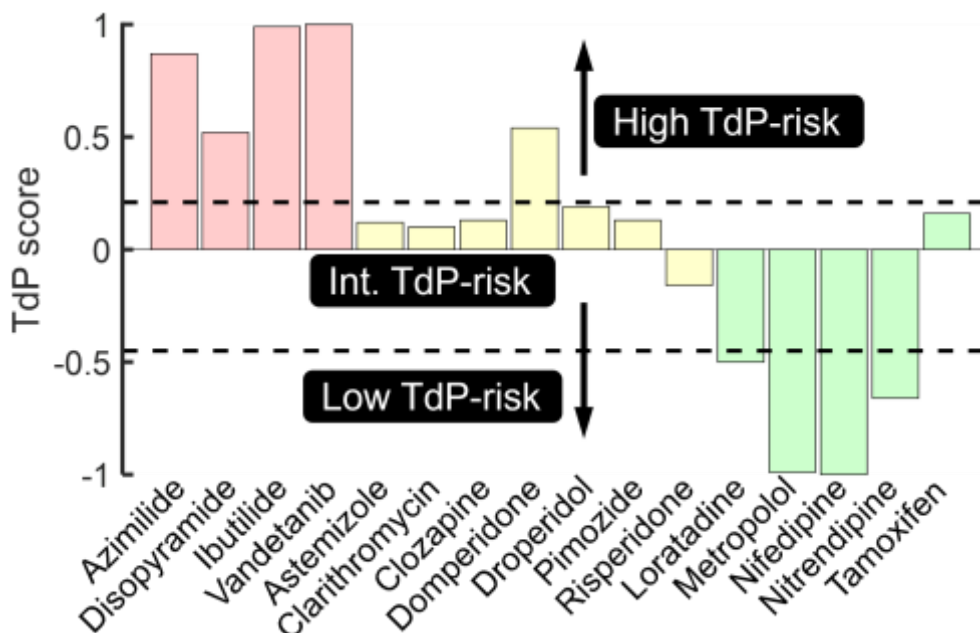316   is due to electrophysiological variability.

Figure 6. Percentage of models predicted as high (red bar), intermediate (yellow bar), or low (green bar) TdP-risk for the 16 validation CiPA drugs using the SVM method on the TorORd population of models. High-risk CiPA drugs are represented at the top, intermediate CiPA drugs in the middle, and low-risk drugs at the bottom.

These percentages were the input for the logistic regression that predicts the overall TdP-risk class of the drug. The output of the logistic regression was summarized in the "TdP-score". TdP-scores for the 16 CiPA validation drugs are shown in **Figure 7**. It can be seen that high-risk drugs have TdP-score values close to 1, intermediate-risk drugs take values close to 0, and low-risk drugs take values close to -1. The thresholds for separation between the three classes were determined in the training phase. For TorORd-population, the optimal threshold between high and intermediate-risk is 0.21 and the optimal threshold between intermediate and low-risk is -0.45. Out of the 16 drugs, 14 are correctly classified with this population-based classifier. The two misclassified drugs are: domperidone, an intermediate-risk drug, which is predicted as a high-risk drug; and tamoxifen, a low-risk drug, that is predicted as an intermediate-risk drug. When testing the classification tool with the 81-drug set from CredibleMeds, 16 drugs were misclassified. Namely, 3 high TdP-risk drugs (cilostazol, dronedarone an procainamide) were classified as intermediate risk drugs. Donepezil, a high TdP-risk drug, was

16

misclassified as a low TdP risk drug. From the intermediate TdP-risk drugs, lapatinib,

nilotinib, paliperidone, sunitinib and tolterodine were predicted as high risk drugs; while

desipramine, saquinavir, famotidine, propafenone and quetiapine were misclassified as

low TdP-risk drugs. Finally, the low risk drugs cibenzoline and darunavir were

miclassified as intermediate risk drugs.

TdP-scores representations for the 81 CredibleMeds drugs for both population of

models (TorORd and ORdmD) are shown in **Figure S7 and S8**.

Figure 7. TdP-score for the 16 CiPA validation drugs simulated on the TorORd
population of models. Actual high-risk CiPA drugs are represented in red bars,
intermediate-risk drugs in yellow and low-risk drugs in green. The dashed lines are the
TdP-score threshold. Threshold1 is equal to 0.21 and all drugs with a higher TdP-score
are predicted as high-risk. Threshold2 is equal to -0.45 and all drugs with a lower TdP-
score are predicted as low-risk. TdP-score values comprised between both thresholds are
considered as intermediate-risk.

The performance of the classifier using TorORd baseline model and the classifier using

the population of TorORd models are shown in **Table 2**. The population-based classifier

outperforms the baseline model-based classifier with both validation datasets. For both

datasets, when using the population of models, the accuracy improves around 20

percentual points and the mean classification error (MCE) is reduced to the half

17

356 approximately. In the case of the CiPA validation dataset, risperidone and droperidol

357 (intermediate-risk drugs) and loratadine and droperidol (low-risk drugs) are classified

358 correctly only if the population of models is used. In the case of the CredibleMeds data

359 set, 7 high-risk, 2 intermediate-risk, and 7 low-risk drugs are misclassified if population

360 of models is not considered. These results reflect the importance of taking into account

361 electrophysiological variability when simulating the effects of drugs. Training and test

362 accuracy of the different classifiers using the population of models are shown in

363 **Supplementary Material**, **Table S5**.

364 **Table 2.** Confusion matrices and performance metrics (accuracy, mean classification
365 error -MCE-, and Matthew correlation coefficient -MCC-) of the classifier using TorORd
366 baseline model and the classifier using the population of TorORd models for both external
367 validation datasets: the 16 CiPA drugs and for the 81 CredibleMeds drugs.

Baseline TorORd model							
CiPA drugs	High	Int.	Low	*CredibleMeds drugs*	High	Int.	Low
Pred. High	4	2	1	**Pred. High**	9	6	0
Pred. Int.	0	4	2	**Pred. Int.**	9	11	9
Pred. Low	0	1	2	**Pred. Low**	2	6	29
Accuracy:	62.5 %			Accuracy:	60.5 %		
MCE:	0.438			MCE:	0.420		
MCC:	0.456			MCC:	0.384		

368

Population of TorORd models							
CiPA drugs	High	Int.	Low	*CredibleMeds drugs*	High	Int.	Low
Pred. High	4	1	0	**Pred. High**	16	5	0
Pred. Int.	0	6	1	**Pred. Int.**	3	13	2
Pred. Low	0	0	4	**Pred. Low**	1	5	36
Accuracy:	87.5 %			Accuracy:	80.2 %		
MCE:	0.125			MCE:	0.210		
MCC:	0.813			MCC:	0.690		

369   Finally, a SFFS algorithm was applied to reduce the number of needed biomarkers.

370 The minimum set of features that maximizes the accuracy of the classifier was the same

371 for ORdmD and TorORd simulations. It was composed of: APD90, qNet, calcium

372   systolic concentration and the electromechanical window. A new classifier was trained

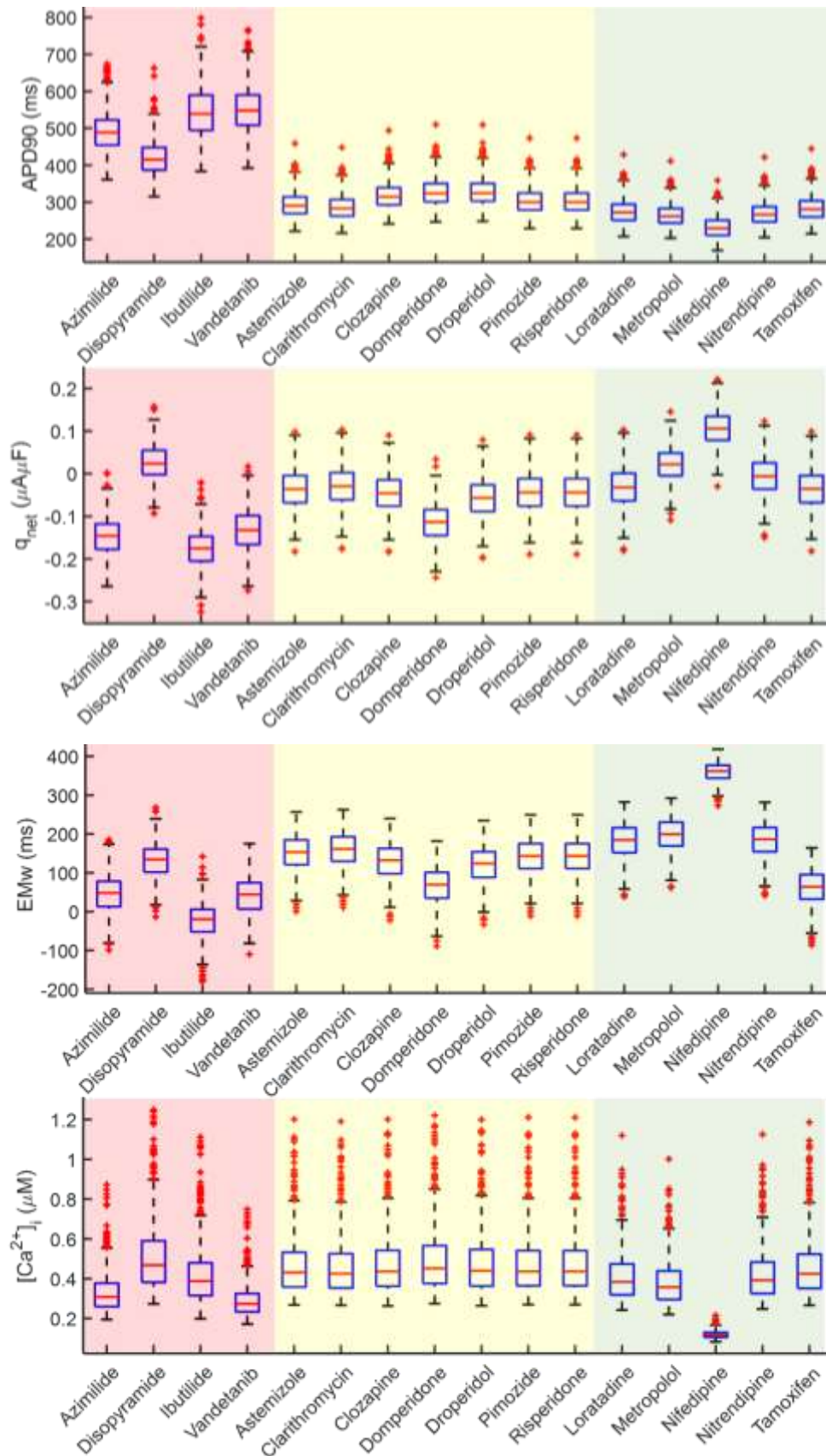373   again, this time using only these 4 features.

374   **Table 3** summarizes performance results of the new classifier that uses only 4 features

375   extracted from a population of TorORd models. For the CiPA dataset, the classifier

376   achieved the same accuracy (87.5%) than in the previous case, using all features. The two

377   misclassified drugs are the same: domperidone and tamoxifen. However, when

378   CredibleMeds data set is used the performance drops slightly. In this case, two more drugs

379   (moxifloxacin - a high-risk drug- and fluvoxamine -an intermediate-risk drug) are

380   misclassified (as intermediate-risk and as high-risk, respectively) thus reducing the

381   accuracy in 2.4% and increasing MCE in 0.02. Despite this, it can be affirmed that the

382   classifier continues to perform with considerable accuracy and that the 4 selected features

383   are able to largely collect the torsadogenic effects of drugs.

384 **Table 3.** Confusion matrices and performance metrics (accuracy, mean classification
385 error -MCE-, and Matthew correlation coefficient -MCC-) of the classifier based on the
386 population of TorORd models, using as inputs: APD90, qNet, EMw, systolic $[Ca^{2+}]_i$.

Population of TorORd models						
CiPA drugs	**High**	**Int.**	**Low**	*CredibleMeds drugs*	**High**	**Int.**	**Low**
Pred. High	4	1	0	**Pred. High**	15	6	0
Pred. Int.	0	6	1	**Pred. Int.**	4	12	2
Pred. Low	0	0	4	**Pred. Low**	1	5	36
Accuracy:	87.5 %			Accuracy:	77.8 %		
MCE:	0.125			MCE:	0.235		
MCC:	0.813			MCC:	0.650		

387   Boxplots of the selected features, at 10 times the EFTPC, are represented in **Figure 8**.

388 In general high-risk drugs greatly prolong APD90. qNet and the EMw follow a similar

389 trend: high-risk drugs tend to decrease their value while low-risk drugs increase them.

390 And regarding systolic calcium concentration, low-risk drugs especially reduce it. It can

391 be observed that, individually, none of the features clearly discriminates between TdP-

392   risk classes, thus it is necessary to combine different biomarkers, and different

393   concentrations must be considered so that the classifier accurately performs.

Figure 8. Box plots of the 4 selected features (APD90, qNet, EMw, systolic Ca²⁺) for at the 16 CiPA validation drugs simulated at 10 times the EFTPC on the population of TorORd models. The red-shaded area includes actual high-risk drugs, the yellow-shaded area the actual intermediate-risk drugs, and the green-shaded area the low-risk drugs.

21

4   Discussion

4.1   Main findings

In this work, we calibrated two population of models (TorORd and ORdmD) to account for electrophysiological variability and we compared the performance of a ternary classification tool, based on SVM, with and without electrophysiological variability. These classifiers were blindly validated, as recommended by Li et al. [7], using the 16 validation CiPA drugs and an extra validation dataset composed of 81 drugs. Our main findings are:

(i)   Populations of models allowed to generate different AP responses under the same pharmacological intervention and to identify ionic conductance profiles more prone to develop TdP. We found that individuals with lower conductances of I_{Kr}, I_{Ks}, I_{NaK}, and I_{Kb} and higher conductances of I_{CaL}, I_{NaL}, and I_{NCX} are more prone to develop TdP.

(ii)   Classification accuracy significantly improves (more than 20 percentual points) when using population of models. This result highlights the benefits of using population of models when predicting TdP-risk and suggest that considering electrophysiological variability has the potential to improve *in silico* TdP-risk assessment tools. Furthermore, the results are similar regardless of the electrophysiological model used (ORdmJ or TorORd). The advantage of using the population of models was also evidenced with the two test datasets used.

(iii)   The feature selection algorithm SFSS revealed the 4 most relevant biomarkers for the prediction of TdP out of the 9 biomarkers studied in this work. These features were: APD90, qNet, systolic calcium concentration and EMw.

421   (iv)   We have defined the TdP_score index, which provides a summarized

422   quantification of the TdP-risk. The most dangerous drugs take values close to 1

423   and the least dangerous close to -1.

4.2 TdP-risk classifiers

425   According to the levels of acceptable performance models defined by Li et al. [30] for

426   CiPA predictive models, the classification tool based on population of TorORd models,

427   which scored the highest performance in this work, presents an "excellent" performance

428   with a MCE lower than 0.3 with both validation datasets. Therefore, it can be said that

429   our models are acceptable for TdP-risk predictions.

430   Regarding the performance comparison of the classification tool, "General Principles"

431   for the validation of TdP-risk prediction models, published by Li's group [7], suggest that

432   prediction models should differentiate between three TdP-risk categories and should be

433   validated with a hidden dataset. However, the authors are aware of only two papers that

434   have been published to date following this suggestion: a work by Li et al. [30], and a

435   recently published paper by Yoo [10]. Furthermore, these are not completely comparable

436   studies, as they do not take into account electrophysiological variability; they quantify

437   the uncertainty in pharmacological values and propagate it through the model. Li et al.

438   [30] proposed a logistic model using the *torsade metric score* (average of qNet across 1-

439   4xCmax). They accurately classified 12 drugs, missing disopyramide, domperidone,

440   clozapine, and risperidone. Yoo et al. [10] proposed an artificial neural network with 9

441   AP-related biomarkers. They also accurately classified 12 drugs out of the 16,

442   misclassifying disopyramide, azimilide, loratadine, and tamoxifen. As previously

443   mentioned, our classification tool misclassifies only 2 drugs out of the 16 CiPA validation

444   drugs (tamoxifen and domperidone) and 16 drugs out of the 81 CredibleMeds drug set.

445   As proposed by Li and colleagues [9], a plausible explanation for the misclassification of

446   these drugs might be technical difficulties for the characterization of drug potency, which

447   leads to mischaracterization of IC_{50}. Another reason for misclassification might be under

448   or overestimation of the role of a specific current of the in silico model, specifically poor

449   representation of the I_{NaL} and I_{CaL} inhibition or overrepresentation of I_{Kr} block effects [31].

450   This might be the case of tamoxifen, which shows similar potencies for I_{Kr}, I_{NaL} and I_{CaL},

451   but the effects captured by the in silico model on I_{CaL} and I_{NaL} seem insufficient to

452   counteract the prolongation of the action potential caused by I_{Kr} block. In addition, other

453   drug-related phenomena such as the effects on other pathways different than ionic

454   channels, trafficking inhibition, the activity of metabolites, or higher concentrations of

455   the compound in the cardiac tissue than in blood plasmas, may impact TdP-risk induction

456   but were not included in our work. These aspect could have favored the misclassification

457   of some drugs. As an example, donepezil prolongs QT interval by I_{Kr} block and also by

458   I_{Kr} trafficking inhibition [32]. Dronedarone is metabolized into N-debutyl-

459   dronedarone[33], a compound that retains up to one-third of the parent's activity. As both

460   have significant channel blocking effects, not considering N-debutyl-dronedarone

461   activity when simulating dronedarone might be the cause of its misclassification.

462   Cilostazol is a phosphodiesterase 3 (PED3) inhibitor that can favor the induction of TdP

463   because it induces intracellular cAMP elevation, which results in Ca^{2+} dynamic

464   disbalance, and early after depolarizations[34]. As for saquinavir, the underestimation of

465   its TdP-risk could be related to the of higher accumulation of the drug in myocardium

466   than in blood plasma [35], increasing the probability of provoking adverse effects in the

467   heart.

468   On the other hand, it should be noted that the ternary-classification tool presented here

469   achieves similar performance to previous TdP-risk assessment studies, where binary

470   classifications were carried out [13,22,24,29,36–40].

471   Furthermore, using populations of models allowed to identify ionic conductance

472   profiles more prone to develop TdP: individuals with lower conductances of I_{Kr}, I_{Ks}, I_{NaK},

473   and I_{Kb} and higher conductances of I_{CaL}, I_{NaL}, and I_{NCX} are more prone to develop TdP.

474   This is in closely agreement with other studies: Britton et al. [6] suggested that decreased

475   I_{NaK}, combined with low I_{Kr}, can increase proarrhythmic-risk of drugs; Passini's [29]

476   group showed that individuals with increased I_{CaL}, I_{NaL}, and I_{NCX} and reduced I_{NaK} were

477   highly vulnerable to drug-induced repolarization abnormalities; Lacerda et al. [41] stated

478   that an enhancement of I_{NaL} plays a relevant role in increased risk of TdP. This

479   information may provide insight about clusters of patients in which the dose of

480   proarrhythmogenic drugs should be avoided or reduced. In fact, this ionic profile is

481   consistent with different conditions or situations that have been associated with an

482   increased incidence of TdP. For example, women, who have higher risk to develop TdP,

483   present lower I_{Kr}, and I_{Ks} [42,43]; or patients with chronic systemic inflammation, which

484   can exacerbate drugs' cardiotoxic effects, have a lower expression of I_{Kr} and a higher

485   expression of I_{CaL} [29]. The utility of population of models to represent

486   electrophysiological variability in *in silico* studies was first introduced by Sobie [45];

487   since then different publications have employed this strategy [24,46–48]. The application

488   of the population of *in silico* models approach is reviewed in [5].

489   **4.3   Limitations of the study**

490   As mentioned in the previous section, one the limitation of this work is the reliability

491   of pharmacological data (IC_{50}, h and EFTPC). Recently, efforts have been made to

492   standardize experimental protocols and increase model prediction accuracy

493   standardization protocols [49,50]. However, these new experimental data are only

494   available for a few drugs. To deal with it, we used a similar approach to previous studies

495   [13,22]: we reduced source variability by considering data from similar experimental

496   conditions and then assumed that the published data represented a distribution of values

497   affected by a random error and the variability due to the experimental conditions. Then,

498   the most representative value considering variability was the median, as it is a robust

499   estimator of the central tendency of a data set. In addition, the present results could be

500   extended in the future by combining the uncertainty quantification in the pharmacological

501   data with the population of models to better understand model's tolerability to input

502   variability. Previous works [51–53] have incorporated methods for quantifying

503   uncertainty in pharmacological data (IC50s and hill coefficients) into the CiPA

504   framework and have demonstrated that they provide valuable information, which can

505   inform in the proarrhythmic evaluation of drugs. Furthermore, if more data on

506   pharmacological hERG binding kinetics were available, it would also be of high interest

507   to simulate drug effects with hERG binding kinetics data, since it could improve the

508   classification performance, as some previous studies have shown [30,54].

509   Another limitation is the dependence of the populations results on the number of models

510   and on the distribution of probability from where the scaling factors are sampled. Here,

511   we consider that an initial population of 1,000 models provides a good balance between

512   having an adequate sample size and avoiding having very similar models that just

513   contribute to increase simulation time. In this sense, we repeated the methodology for

514   building the classifiers but starting from a population of 5,000 initial models in order to

515   study if classification results were convergent. For both populations of models (ORdmJ

516   and TorORd), we found that the final drug classification (based on the TdP-score) was

517   the same with the population of 5,000 models and with the population of 1,000 models,

518   although the percentage of models in each category was slightly different. The

519   distributions of the biomarkers used for the calibration across each population (TorORd

520   and ORdmD) with 5,000 initial models, can be consulted in the **Supplementary**

521   **Material,** F**igures S9 and S10**. Furthermore, comparison between the classification

522   results for the 16 CiPA drugs when using an initial population of 5,000 TorORd models

523   or an initial 1,000 TorORd models is shown in **Supplementary Material, Table S6**. On

524   the other hand, we chose a normal distribution since the aim of the study was to predict

525   drugs effects in a healthy population, where ionic conductances are supposed to be a

526   continuum of values normally distributed. In addition, population variability was

527   considered only in ionic current conductances because it constitutes the major

528   determinant behind physiological variability [55]. Another limitation is precisely that

529   drug effects were only simulated on healthy cardiomyocytes, and the incidence of TdP is

530   known to be very rare in this population.

531   It is worth noting that the methodology used here does not seek for the identifiability

532   of the ion channel conductances. Therefore, the scaling factors in the populations of

533   models do no necessarily represent the real variation of ionic conductances responsible

534   for experimentally observed AP. Different strategies for the identifiability of the

535   parameters of the AP model are presented in the review by Whittaker and colleagues [56].

536   On the other hand, regarding the rate dependence, in this study we performed

537   simulations at an intermediate and physiological-like heart rate (60 beats per minutes) as

538   a first approximation. The study of the performance dependence on the stimulation rate

539   could help refine the classification tool. According to some authors, the best

540   discrimination between TdP-risk categories is achieved at stimulations of 1Hz [37,57];

541   instead, Dutta and colleagues observed the best category separation at slower rates (0.5

542   Hz) [54]; while other authors have not found any rate dependence in their classification

543   results [22].

544   Another limitation of this work is the strong dependence of classification performance

545   on the information taken as reference. Here, for the validation drugs not included in the

546   CiPA reference list we used the CredibleMeds database [25]. Although it is a well

547   recognized database which feeds from clinical data, it mixes the QT prolongation and the

548   TdP risk end points. QT prolongation is closely related to but distinct from TdP end point,

549   and inferring TdP risk only from QT interval is inaccurate[7]. In this sense, CredibleMeds

550   class 2 ("possible risk of TdP"), which here was considered as intermediate risk of TdP

551   for the classifiers development, includes compounds that can cause QT prolongation in

552   the absence of evidence for a risk of TdP. Therefore, some of the CredibleMeds validation

553   drugs in the intermediate TdP-risk class actually might have no known risk of TdP and

554   should have been considered as low TdP-risk instead. This could explain the lower

555   performance among all the classifiers when validated with the CredibleMeds dataset.

556   It is to be noted that our simulations do not consider other pharmacological aspects such

557   as drug interactions, effects of active metabolites or accumulation of drugs in cardiac

558   tissues, etc.

559   **5   Conclusions**

560   In this work, we developed a ternary-classification tool based on population of models

561   for the assessment of drug-induced TdP. This tool quantifies the percentage of models in

562   which the drug will be dangerous and summarizes the risk of TdP in the biomarker "TdP

563   score". The validation of the classification tool with two different "hidden" drug sets

564   showed that its performance was higher than when just using the baseline model.

565   Simulations with population of models also allowed the identification of individuals

566   which are more prone to develop TdP. Taken together, the results outline the benefits of

567   using population of models when predicting TdP-risk and suggest that considering

568 electrophysiological variability has the potential to improve *in silico* TdP-risk assessment
569 tools.

570 The methodology presented in this study provides new opportunities to assess drug-
571 induced TdP, taking into account electrophysiolocial variability. The use of such *in silico*
572 tools as screening methods could be helpful to accelerate the development of new drugs
573 and reduce the costs of cardiac safety screening in preclinical phases.

574 **6   Abbreviations used**

575 AP, action potencial; APDx; action potential duration at x% of the repolarization; BCL,
576 basic length cycle; EAD, early after depolarization; EFTPC, effective free therapeutic
577 plasma concentration (peak); EMw, electromechanical window; IC_{50}, half-maximal
578 inhibitory concentration; MCE, mean classification error; MCC, Mathews correlation
579 coefficient; SVM, support vector machines; TdP, Torsade de Pointes.

580 **7   Conflict of interest statement**

581 The authors declare that the research was conducted in the absence of any commercial
582 or financial relationships.

583 **8   Author Contributions**

584 JL contributed to the design of the study, performed the simulations, analyzed results
585 and wrote the first draft of the manuscript. BT and JS contributed to the design of the
586 study, analyzed the results and supervised the project. All authors contributed to
587 manuscript revision, read and approved the submitted version.

588

589

598   **10   Appendix**

599   Population of models parameter sets, the ORdmD CellML file and MALTAB code used

600   in this work are available at: https://riunet.upv.es/handle/10251/182593

601   **11   References**

602   [1]   B. Fermini, J.C. Hancox, N. Abi-Gerges, M. Bridgland-Taylor, K.W. Chaudhary,
603   T. Colatsky, K. Correll, W. Crumb, B. Damiano, G. Erdemli, G. Gintant, J.
604   Imredy, J. Koerner, J. Kramer, P. Levesque, Z. Li, A. Lindqvist, C.A. Obejero-
605   Paz, D. Rampe, K. Sawada, D.G. Strauss, J.I. Vandenberg, A new perspective in
606   the field of cardiac safety testing through the comprehensive in vitro
607   proarrhythmia assay paradigm, Journal of Biomolecular Screening. 21 (2016) 1–
608   11. https://doi.org/10.1177/1087057115594589.

609   [2]   P.T. Sager, G. Gintant, J.R. Turner, S. Pettit, N. Stockbridge, Rechanneling the
610   cardiac proarrhythmia safety paradigm: A meeting report from the Cardiac Safety
611   Research Consortium, American Heart Journal. 167 (2014) 292–300.
612   https://doi.org/10.1016/j.ahj.2013.11.004.

613   [3]   J.S. Park, J.Y. Jeon, J.H. Yang, M.G. Kim, Introduction to in silico model for
614   proarrhythmic risk assessment under the CiPA initiative, Translational and
615   Clinical Pharmacology. 27 (2019) 12–18.
616   https://doi.org/10.12793/TCP.2019.27.1.12.

617   [4]   H. Ni, S. Morotti, E. Grandi, A heart for diversity: Simulating variability in
618   cardiac arrhythmia research, Frontiers in Physiology. 9 (2018) 1–19.
619   https://doi.org/10.3389/fphys.2018.00958.

620 [5] A. Muszkiewicz, O.J. Britton, P. Gemmell, E. Passini, C. Sánchez, X. Zhou, A.
621   Carusi, T.A. Quinn, K. Burrage, A. Bueno-Orovio, B. Rodriguez, Variability in
622   cardiac electrophysiology: Using experimentally-calibrated populations of
623   models to move beyond the single virtual physiological human paradigm, Prog
624   Biophys Mol Biol. 120 (2016) 115–127.
625   https://doi.org/10.1016/J.PBIOMOLBIO.2015.12.002.

626 [6] O.J. Britton, A. Bueno-Orovio, L. Virág, A. Varró, B. Rodriguez, The
627   electrogenic Na+/K+ pump is a key determinant of repolarization abnormality
628   susceptibility in human ventricular cardiomyocytes: A population-based
629   simulation study, Frontiers in Physiology. 8 (2017).
630   https://doi.org/10.3389/fphys.2017.00278.

631 [7] Z. Li, G.R. Mirams, T. Yoshinaga, B.J. Ridder, X. Han, J.E. Chen, N.L.
632   Stockbridge, T.A. Wisialowski, B. Damiano, S. Severi, P. Morissette, P.R.
633   Kowey, M. Holbrook, G. Smith, R.L. Rasmusson, M. Liu, Z. Song, Z. Qu, D.J.
634   Leishman, J. Steidl-Nichols, B. Rodriguez, A. Bueno-Orovio, X. Zhou, E.
635   Passini, A.G. Edwards, S. Morotti, H. Ni, E. Grandi, C.E. Clancy, J. Vandenberg,
636   A. Hill, M. Nakamura, T. Singer, L. Polonchuk, A. Greiter-Wilke, K. Wang, S.
637   Nave, A. Fullerton, E.A. Sobie, M. Paci, F. Musuamba Tshinanu, D.G. Strauss,
638   General Principles for the Validation of Proarrhythmia Risk Prediction Models:
639   An Extension of the CiPA In Silico Strategy, Clinical Pharmacology and
640   Therapeutics. 107 (2020) 102–111. https://doi.org/10.1002/cpt.1647.

641 [8] G.R. Mirams, Y. Cui, A. Sher, M. Fink, J. Cooper, B.M. Heath, N.C. McMahon,
642   D.J. Gavaghan, D. Noble, Simulation of multiple ion channel block provides
643   improved early prediction of compounds' clinical torsadogenic risk., Cardiovasc
644   Res. 91 (2011) 53–61. https://doi.org/10.1093/cvr/cvr044.

645 [9] Z. Li, B.J. Ridder, X. Han, W.W. Wu, J. Sheng, P.N. Tran, M. Wu, A. Randolph,
646   R.H. Johnstone, G.R. Mirams, Y. Kuryshev, J. Kramer, C. Wu, W.J. Crumb,
647   D.G. Strauss, Assessment of an In Silico Mechanistic Model for Proarrhythmia
648   Risk Prediction Under the CiPA Initiative, Clin Pharmacol Ther. 105 (2019)
649   466–475. https://doi.org/10.1002/CPT.1184.

650 [10] Y. Yoo, A. Marcellinus, D.U. Jeong, K.-S. Kim, K.M. Lim, Assessment of Drug
651   Proarrhythmicity Using Artificial Neural Networks With in silico Deterministic
652   Model Outputs, Frontiers in Physiology. 0 (2021) 2289.
653   https://doi.org/10.3389/FPHYS.2021.761691.

654 [11] J. Tomek, A. Bueno-Orovio, B. Rodriguez, ToR-ORd-dynCl: an update of the
655   ToR-ORd model of human ventricular cardiomyocyte with dynamic intracellular
656   chloride, BioRxiv. (2020) 2020.06.01.127043.
657   https://doi.org/10.1101/2020.06.01.127043.

658 [12] T. O'Hara, L. Virág, A. Varró, Y. Rudy, Simulation of the Undiseased Human
659   Cardiac Ventricular Action Potential: Model Formulation and Experimental
660   Validation, PLoS Computational Biology. 7 (2011) e1002061.
661   https://doi.org/10.1371/journal.pcbi.1002061.

662   [13] J. Llopis-Lorente, J. Gomis-Tena, J. Cano, L. Romero, J. Saiz, B. Trenor, In
663   silico classifiers for the assessment of drug proarrhythmicity, Journal of
664   Chemical Information and Modeling. 60 (2020) 5172–5187.
665   https://doi.org/10.1021/acs.jcim.0c00201.

666   [14] C. A, G. W, R. B, Ionic mechanisms of electrophysiological properties and
667   repolarization abnormalities in rabbit Purkinje fibers, Am J Physiol Heart Circ
668   Physiol. 300 (2011). https://doi.org/10.1152/AJPHEART.01170.2010.

669   [15] R. L, P. E, F. M, R. B, Impact of ionic current variability on human ventricular
670   cellular electrophysiology, Am J Physiol Heart Circ Physiol. 297 (2009).
671   https://doi.org/10.1152/AJPHEART.00263.2009.

672   [16] D.A. Sampedro, Theoretical Analysis of Autonomic Nervous System Effects on
673   Cardiac Electrophysiology an its Relationship with the Arrhythmias Risk, 2020.

674   [17] U. Schmidt, R.J. Hajjar, P.A. Helm, C.S. Kim, A.A. Doye, J.K. Gwathmey,
675   Contribution of abnormal sarcoplasmic reticulum ATPase activity to systolic and
676   diastolic dysfunction in human heart failure, Journal of Molecular and Cellular
677   Cardiology. 30 (1998) 1929–1937. https://doi.org/10.1006/jmcc.1998.0748.

678   [18] E. Grandi, F.S. Pasqualini, D.M. Bers, A novel computational model of the
679   human ventricular action potential and Ca transient, Journal of Molecular and
680   Cellular Cardiology. 48 (2010) 112–121.
681   https://doi.org/10.1016/J.YJMCC.2009.09.019.

682   [19] B. Pieske, L.S. Maier, V. Piacentino, J. Weisser, G. Hasenfuss, S. Houser, Rate
683   dependence of [Na+]i and contractility in nonfailing and failing human
684   myocardium, Circulation. 106 (2002) 447–453.
685   https://doi.org/10.1161/01.CIR.0000023042.50192.F4.

686   [20] R. Coppini, C. Ferrantini, L. Yao, P. Fan, M. del Lungo, F. Stillitano, L. Sartiani,
687   B. Tosi, S. Suffredini, C. Tesi, M. Yacoub, I. Olivotto, L. Belardinelli, C.
688   Poggesi, E. Cerbai, A. Mugelli, Late sodium current inhibition reverses
689   electromechanical dysfunction in human hypertrophic cardiomyopathy,
690   Circulation. 127 (2013) 575–584.
691   https://doi.org/10.1161/CIRCULATIONAHA.112.134932.

692   [21] T. Colatsky, B. Fermini, G. Gintant, J.B. Pierson, P. Sager, Y. Sekino, D.G.
693   Strauss, N. Stockbridge, The Comprehensive in Vitro Proarrhythmia Assay
694   (CiPA) initiative — Update on progress, Journal of Pharmacological and
695   Toxicological Methods. 81 (2016) 15–20.
696   https://doi.org/10.1016/j.vascn.2016.06.002.

697   [22] L. Romero, J. Cano, J. Gomis-Tena, B. Trenor, F. Sanz, M. Pastor, J. Saiz, In
698   Silico QT and APD Prolongation Assay for Early Screening of Drug-Induced
699   Proarrhythmic Risk, Journal of Chemical Information and Modeling. 58 (2018)
700   867–878. https://doi.org/10.1021/acs.jcim.7b00440.

701   [23] S. Dutta, D. Strauss, T. Colatsky, Z. Li, Optimization of an In Silico Cardiac Cell
702   Model for Proarrhythmia Risk Assessment, in: 2016 Computing in Cardiology

703   Conference (CinC), 2016: pp. 869–872. https://doi.org/10.22489/CinC.2016.253-
704   483.

705 [24] E. Passini, C. Trovato, P. Morissette, F. Sannajust, A. Bueno-Orovio, B.
706   Rodriguez, Drug-induced shortening of the electromechanical window is an
707   effective biomarker for in silico prediction of clinical risk of arrhythmias, British
708   Journal of Pharmacology. 176 (2019) 3819–3833.
709   https://doi.org/10.1111/bph.14786.

710 [25] R. Woosley, K. Romero, W. Heise, Risk Categories for Drugs that Prolong Qt &
711   Induce Torsade de Pointes (TdP), (n.d.). https://www.crediblemeds.org/druglist
712   (accessed December 14, 2021).

713 [26] J. Pearl, Heuristics: intelligent search strategies for computer problem solving.,
714   Addison-Wesley Longman PublishingCo. Inc, Boston, MA, 1984.

715 [27] V.D.A. Corino, E. Montin, A. Messina, P.G. Casali, A. Gronchi, A. Marchianò,
716   L.T. Mainardi, Radiomic analysis of soft tissues sarcomas can distinguish
717   intermediate from high-grade lesions, J Magn Reson Imaging. 47 (2018) 829–
718   840. https://doi.org/10.1002/JMRI.25791.

719 [28] J.F. Gomez, K. Cardona, L. Romero, J.M. Ferrero, B. Trenor,
720   Electrophysiological and structural remodeling in heart failure modulate
721   arrhythmogenesis. 1D simulation study, PLoS ONE. 9 (2014).
722   https://doi.org/10.1371/journal.pone.0106602.

723 [29] E. Passini, O.J. Britton, H.R. Lu, J. Rohrbacher, A.N. Hermans, D.J. Gallacher,
724   R.J.H. Greig, A. Bueno-Orovio, B. Rodriguez, Human in silico drug trials
725   demonstrate higher accuracy than animal models in predicting clinical pro-
726   arrhythmic cardiotoxicity, Frontiers in Physiology. 8 (2017) 668.
727   https://doi.org/10.3389/fphys.2017.00668.

728 [30] Z. Li, B.J. Ridder, X. Han, W.W. Wu, J. Sheng, P.N. Tran, M. Wu, A. Randolph,
729   R.H. Johnstone, G.R. Mirams, Y. Kuryshev, J. Kramer, C. Wu, W.J. Crumb,
730   D.G. Strauss, Assessment of an In Silico Mechanistic Model for Proarrhythmia
731   Risk Prediction Under the CiPA Initiative, Clin Pharmacol Ther. 105 (2019)
732   466–475. https://doi.org/10.1002/CPT.1184.

733 [31] O.J. Britton, N. Abi-Gerges, G. Page, A. Ghetti, P.E. Miller, B. Rodriguez,
734   Quantitative comparison of effects of dofetilide, sotalol, quinidine, and verapamil
735   between human ex vivo trabeculae and in silico ventricular models incorporating
736   inter-individual action potential variability, Frontiers in Physiology. 8 (2017)
737   597. https://doi.org/10.3389/fphys.2017.00597.

738 [32] L. Cubeddu, Drug-induced Inhibition and Trafficking Disruption of ion
739   Channels: Pathogenesis of QT Abnormalities and Drug-induced Fatal
740   Arrhythmias, Current Cardiology Reviews. 12 (2016) 141–154.
741   https://doi.org/10.2174/1573403x12666160301120217.

742 [33] F. Iram, S. Ali, A. Ahmad, S.A. Khan, A. Husain, A review on dronedarone:
743   Pharmacological, pharmacodynamic and pharmacokinetic profile, Journal of
744   Acute Disease. 5 (2016) 102–108. https://doi.org/10.1016/j.joad.2015.10.002.

745 [34] N. Kanlop, S. Chattipakorn, N. Chattipakorn, Effects of cilostazol in the heart, J
746   Cardiovasc Med (Hagerstown). 12 (2011) 88–95.
747   https://doi.org/10.2459/JCM.0B013E3283439746.

748 [35] X. Zhang, P. Jordan, L. Cristea, M. Salgo, R. Farha, S. Kolis, L.S. Lee, Thorough
749   QT/QTc study of ritonavir-boosted saquinavir following multiple-dose
750   administration of therapeutic and supratherapeutic doses in healthy participants, J
751   Clin Pharmacol. 52 (2012) 520–529. https://doi.org/10.1177/0091270011400071.

752 [36] L.J. Cantilena, J. Koerner, R. Temple, D. Throckmorton, FDA evaluation of
753   cardiac repolarization data for 19 drugs and drug candidates, Clinical
754   Pharmacology & Therapeutics. 79 (2006) P29–P29.
755   https://doi.org/10.1016/j.clpt.2005.12.106.

756 [37] J. Parikh, V. Gurev, J.J. Rice, Novel two-step classifier for Torsades de Pointes
757   risk stratification from direct features, Frontiers in Pharmacology. 8 (2017) 816.
758   https://doi.org/10.3389/fphar.2017.00816.

759 [38] J. Kramer, C.A. Obejero-Paz, G. Myatt, Y.A. Kuryshev, A. Bruening-Wright,
760   J.S. Verducci, A.M. Brown, MICE models: Superior to the HERG model in
761   predicting torsade de pointes, Scientific Reports. 3 (2013) 2100.
762   https://doi.org/10.1038/srep02100.

763 [39] W.S. Redfern, L. Carlsson, A.S. Davis, W.G. Lynch, I. MacKenzie, S.
764   Palethorpe, P.K.S. Siegl, I. Strang, A.T. Sullivan, R. Wallis, A.J. Camm, T.G.
765   Hammond, Relationships between preclinical cardiac electrophysiology, clinical
766   QT interval prolongation and torsade de pointes for a broad range of drugs:
767   Evidence for a provisional safety margin in drug development, Cardiovascular
768   Research. 58 (2003) 32–45. https://doi.org/10.1016/S0008-6363(02)00846-5.

769 [40] X. Zhou, Y. Qu, E. Passini, A. Bueno-Orovio, Y. Liu, H.M. Vargas, B.
770   Rodriguez, Blinded In Silico Drug Trial Reveals the Minimum Set of Ion
771   Channels for Torsades de Pointes Risk Assessment, Frontiers in Pharmacology.
772   10 (2020) 1643. https://doi.org/10.3389/fphar.2019.01643.

773 [41] A.E. Lacerda, Y.A. Kuryshev, Y. Chen, M. Renganathan, H. Eng, S.J. Danthi,
774   J.W. Kramer, T. Yang, A.M. Brown, Alfuzosin delays cardiac repolarization by a
775   novel mechanism, Journal of Pharmacology and Experimental Therapeutics. 324
776   (2008) 427–433. https://doi.org/10.1124/jpet.107.128405.

777 [42] W. Yang, N.M. Warrington, S.J. Taylor, P. Whitmire, E. Carrasco, K.W.
778   Singleton, N. Wu, J.D. Lathia, M.E. Berens, A.H. Kim, J.S. Barnholtz-Sloan,
779   K.R. Swanson, J. Luo, J.B. Rubin, Sex differences in GBM revealed by analysis
780   of patient imaging, transcriptome, and survival data, Sci Transl Med. 11 (2019).
781   https://doi.org/10.1126/SCITRANSLMED.AAO5253.

782 [43] A. Fogli Iseppe, H. Ni, S. Zhu, X. Zhang, R. Coppini, P.C. Yang, U. Srivatsa,
783   C.E. Clancy, A.G. Edwards, S. Morotti, E. Grandi, Sex-Specific Classification of
784   Drug-Induced Torsade de Pointes Susceptibility Using Cardiac Simulations and
785   Machine Learning, Clinical Pharmacology & Therapeutics. 110 (2021) 380–391.
786   https://doi.org/10.1002/CPT.2240.

787   [44]   C. Campana, R. Dariolli, M. Boutjdir, E.A. Sobie, Inflammation as a Risk Factor
788   in Cardiotoxicity: An Important Consideration for Screening During Drug
789   Development, Frontiers in Pharmacology. 12 (2021) 845.
790   https://doi.org/10.3389/FPHAR.2021.598549/BIBTEX.

791   [45]   E.A. Sobie, Parameter sensitivity analysis in electrophysiological models using
792   multivariable regression, Biophysical Journal. 96 (2009) 1264–1274.
793   https://doi.org/10.1016/j.bpj.2008.10.056.

794   [46]   M. Paci, E. Passini, S. Severi, J. Hyttinen, B. Rodriguez, Phenotypic variability
795   in LQT3 human induced pluripotent stem cell-derived cardiomyocytes and their
796   response to antiarrhythmic pharmacologic therapy: An in silico approach, Heart
797   Rhythm. 14 (2017) 1704–1712. https://doi.org/10.1016/J.HRTHM.2017.07.026.

798   [47]   M. Varshneya, I. Irurzun-Arana, C. Campana, R. Dariolli, A. Gutierrez, T.K.
799   Pullinger, E.A. Sobie, Investigational Treatments for COVID-19 may Increase
800   Ventricular Arrhythmia Risk Through Drug Interactions, CPT Pharmacometrics
801   Syst Pharmacol. 10 (2021) 100–107. https://doi.org/10.1002/PSP4.12573.

802   [48]   P. Morissette, S. Polak, A. Chain, J. Zhai, J.P. Imredy, M.J. Wildey, J. Travis, K.
803   Fitzgerald, P. Fanelli, E. Passini, B. Rodriguez, F. Sannajust, C. Regan,
804   Combining an in silico proarrhythmic risk assay with a tPKPD model to predict
805   QTc interval prolongation in the anesthetized guinea pig assay, Toxicology and
806   Applied Pharmacology. 390 (2020).
807   https://doi.org/10.1016/J.TAAP.2020.114883.

808   [49]   J. Gomis-Tena, B.M. Brown, J. Cano, B. Trenor, P.-C. Yang, J. Saiz, C.E.
809   Clancy, L. Romero, When Does the IC 50 Accurately Assess the Blocking
810   Potency of a Drug?, Cite This: J. Chem. Inf. Model. 2020 (2020) 1779–1790.
811   https://doi.org/10.1021/acs.jcim.9b01085.

812   [50]   B.J. Ridder, D.J. Leishman, M. Bridgland-Taylor, M. Samieegohar, X. Han,
813   W.W. Wu, A. Randolph, P. Tran, J. Sheng, T. Danker, A. Lindqvist, D. Konrad,
814   S. Hebeisen, L. Polonchuk, E. Gissinger, M. Renganathan, B. Koci, H. Wei, J.
815   Fan, P. Levesque, J. Kwagh, J. Imredy, J. Zhai, M. Rogers, E. Humphries, R.
816   Kirby, S. Stoelzle-Feix, N. Brinkwirth, M.G. Rotordam, N. Becker, S. Friis, M.
817   Rapedius, T.A. Goetze, T. Strassmaier, G. Okeyo, J. Kramer, Y. Kuryshev, C.
818   Wu, H. Himmel, G.R. Mirams, D.G. Strauss, R. Bardenet, Z. Li, A systematic
819   strategy for estimating hERG block potency and its implications in a new cardiac
820   safety paradigm, Toxicology and Applied Pharmacology. 394 (2020) 114961.
821   https://doi.org/10.1016/j.taap.2020.114961.

822   [51]   R.C. Elkins, M.R. Davies, S.J. Brough, D.J. Gavaghan, Y. Cui, N. Abi-Gerges,
823   G.R. Mirams, Variability in high-throughput ion-channel screening data and
824   consequences for cardiac safety assessment, Journal of Pharmacological and
825   Toxicological Methods. 68 (2013) 112–122.
826   https://doi.org/10.1016/J.VASCN.2013.04.007.

827   [52]   R.H. Johnstone, R. Bardenet, D.J. Gavaghan, G.R. Mirams, J. Stott, D.
828   Leishman, Hierarchical Bayesian inference for ion channel screening dose-

829   response data, Wellcome Open Research 2017 1:6. 1 (2017) 6.
830   https://doi.org/10.12688/wellcomeopenres.9945.2.

831   [53] K.C. Chang, S. Dutta, G.R. Mirams, K.A. Beattie, J. Sheng, P.N. Tran, M. Wu,
832   W.W. Wu, T. Colatsky, D.G. Strauss, Z. Li, Uncertainty quantification reveals
833   the importance of data variability and experimental design considerations for in
834   silico proarrhythmia risk assessment, Frontiers in Physiology. 8 (2017) 917.
835   https://doi.org/10.3389/FPHYS.2017.00917/BIBTEX.

836   [54] S. Dutta, K.C. Chang, K.A. Beattie, J. Sheng, P.N. Tran, W.W. Wu, M. Wu, D.G.
837   Strauss, T. Colatsky, Z. Li, Optimization of an in silico cardiac cell model for
838   proarrhythmia risk assessment, Frontiers in Physiology. 8 (2017) 616.
839   https://doi.org/10.3389/fphys.2017.00616.

840   [55] O.J. Britton, A. Bueno-Orovio, K. van Ammel, H.R. Lu, R. Towart, D.J.
841   Gallacher, B. Rodriguez, Experimentally calibrated population of models predicts
842   and explains intersubject variability in cardiac cellular electrophysiology, Proc
843   Natl Acad Sci U S A. 110 (2013) E2098–E2105.
844   https://doi.org/10.1073/pnas.1304382110.

845   [56] D.G. Whittaker, M. Clerx, C.L. Lei, D.J. Christini, G.R. Mirams, Calibration of
846   ionic and cellular cardiac electrophysiology models, Wiley Interdisciplinary
847   Reviews: Systems Biology and Medicine. 12 (2020) e1482.
848   https://doi.org/10.1002/WSBM.1482.

849   [57] M.C. Lancaster, E.A. Sobie, Improved Prediction of Drug-Induced Torsades de
850   Pointes Through Simulations of Dynamics and Machine Learning Algorithms,
851   Clin Pharmacol Ther. 100 (2016) 371–379. https://doi.org/10.1002/CPT.367.

852